

# Fluorescence Array-Based Sensing of Metal Ions Using Conjugated Polyelectrolytes

Yi Wu,<sup>†,‡</sup> Ying Tan,<sup>‡</sup> Jiatao Wu,<sup>†,‡</sup> Shangying Chen,<sup>§</sup> Yu Zong Chen,<sup>§,||</sup> Xinwen Zhou,<sup>⊥</sup> Yuyang Jiang,<sup>\*,‡</sup> and Chunyan Tan<sup>\*,‡</sup>

<sup>†</sup>Department of Chemistry, Tsinghua University, Beijing 100084, P. R. China

<sup>‡</sup>The Ministry-Province Jointly Constructed Base for State Key Lab- Shenzhen Key Laboratory of Chemical Biology, the Graduate School at Shenzhen, Tsinghua University, Shenzhen 518055, P. R. China

<sup>§</sup>Bioinformatics and Drug Design Group, Department of Pharmacy, National University of Singapore, Singapore 117543, Singapore

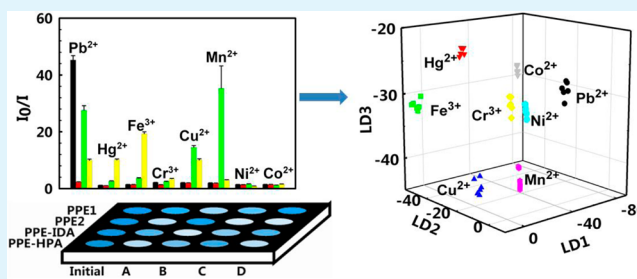
<sup>||</sup>Shenzhen Kivita Innovative Drug Discovery Institute, Shenzhen 518055, P. R. China

<sup>⊥</sup>Institute of Biomedical Sciences, Fudan University, Shanghai 200433, P. R. China

## Supporting Information

**ABSTRACT:** Array-based sensing offers several advantages for detecting a series of analytes with common structures or properties. In this study, four anionic conjugated polyelectrolytes (CPEs) with a common poly(*p*-phenylene ethynylene) (PPE) backbone and varying pendant ionic side chains were designed. The conjugation length, repeat unit pattern, and ionic side chain composition were the main factors affecting the fluorescence patterns of CPE polymers in response to the addition of different metal ions. Eight metal ions, including  $\text{Pb}^{2+}$ ,  $\text{Hg}^{2+}$ ,  $\text{Fe}^{3+}$ ,  $\text{Cr}^{3+}$ ,  $\text{Cu}^{2+}$ ,  $\text{Mn}^{2+}$ ,  $\text{Ni}^{2+}$ , and  $\text{Co}^{2+}$ , categorized as water contaminants by the Environmental Protection Agency, were selected as analytes in this study. Fluorescence intensity response patterns of the four-PPE sensor array toward each of the metal ions were recorded, analyzed, and transformed into canonical scores using linear discrimination analysis (LDA), which permitted clear differentiation between metal ions using both two-dimensional and three-dimensional graphs. In particular, the array could readily differentiate between eight toxic metal ions in separate aqueous solutions at 100 nM. Our four-PPE sensor array also provides a practical application to quantify  $\text{Pb}^{2+}$  and  $\text{Hg}^{2+}$  concentrations in blind samples within a specific concentration range.

**KEYWORDS:** conjugated polyelectrolytes, poly(*p*-phenylene ethynylene), sensor array, metal ion, LDA



## INTRODUCTION

Since the beginning of industrialization, heavy metal pollution in water and soil sources has remained a major problem that negatively impacts human health and sustainable development.<sup>1</sup> Although commonly used methods such as atomic absorption spectrometry and inductively coupled plasma mass spectrometry (MS) have provided accurate measurements of metal ions,<sup>2,3</sup> the inconvenience, inflexibility for use in on-site analysis, and high cost of these methods impede their use. Therefore, convenient detection and quantification of heavy metal ions have always been of great interest to researchers. Fluorescent detection methods offer a cost-effective alternative for counteracting these limitations but require the design and synthesis of sensor molecules with high specificity for each analyte to be detected. Therefore, this approach is challenging and time-consuming for the analysis of several structurally similar analytes. Alternatively, array-based approaches have emerged to analyze biological macromolecules, contaminants, bacteria, food additives, and metal ions<sup>4–13</sup> and use an array of sensors instead of a one-sensor-per-analyte scheme. Thus, differentiation among a series of analytes can be achieved by

exploiting the distinct response patterns produced for each analyte from the combined effect of all of the sensors in the array.

Conjugated polyelectrolytes (CPEs) are water-soluble conjugated polymers with ionic side chains.<sup>14–19</sup> CPEs feature a molecular wire effect and are sensitive to minor conformational or environmental changes,<sup>20–22</sup> which make them excellent sensing materials for proteins, DNAs, small molecules, and others.<sup>23–27</sup> Array-based sensors constructed from several CPEs have been used to study proteins, cells, and bacteria.<sup>23,28–33</sup> Using a sensor array consisting of seven conjugated polymers that were soluble in organic solvents (tetrahydrofuran (THF) and chloroform), differentiation between seven metal ions was achieved using direct comparison via visual discrimination of the patterns produced by the polymers' fluorescence intensity changes.<sup>34</sup>

Received: January 20, 2015

Accepted: March 5, 2015

Published: March 5, 2015

In this study, we designed and synthesized four anionic CPEs that share a poly(paraphenylene ethynylene) (PPE) backbone but were modified with different pendant ionic side chains. These CPEs were shown to bind to metal ions with varying selectivities to give rise to distinct fluorescence responses via polymer–metal ion interactions. Structural and photophysical characterization of the four CPEs were performed, and these polymers were used to create a four-PPE sensor array. After separate addition of eight different metal ions, the fluorescence intensity responses were measured for the sensor array. The fluorescence patterns were constructed and transformed into canonical scores by means of linear discrimination analysis (LDA), permitting a clear observation of the differentiation between metal ions. Furthermore, our four-PPE sensor array was shown to provide a practical application to quantify the concentration of  $\text{Pb}^{2+}$  and  $\text{Hg}^{2+}$ , important environmental pollutants, within a certain concentration range.

## ■ EXPERIMENTAL SECTION

**Materials.** Bis(triphenylphosphine) palladium chloride ( $\text{PdCl}_2(\text{PPh}_3)_2$ ), tetrakis(triphenylphosphine) palladium ( $\text{Pd}(\text{PPh}_3)_4$ ), and cuprous iodide (CuI) were purchased from Aladdin Chemical Co. (Shanghai, China) and used as received. Nitromethane, iminodiacetic acid diethyl ester, and *tert*-butyl acrylate were purchased from JK Chemical (Beijing, China) and used without further purification. THF was dried by distillation from sodium metal and kept under argon before use. Metal compounds at analytical reagent or higher grade were purchased from different suppliers and used as received unless otherwise noted. Manganese sulfate monohydrate ( $\text{MnSO}_4 \cdot \text{H}_2\text{O}$ ), lead nitrate ( $\text{Pb}(\text{NO}_3)_2$ ), mercuric sulfate ( $\text{HgSO}_4$ ), cobalt chloride hexahydrate ( $\text{CoCl}_2 \cdot 6\text{H}_2\text{O}$ ), nickel sulfate hexahydrate ( $\text{NiSO}_4 \cdot 6\text{H}_2\text{O}$ ), and ferrous chloride hexahydrate ( $\text{FeCl}_2 \cdot 6\text{H}_2\text{O}$ ) were purchased from Aladdin Chemical Co. (Shanghai, China). Copper chloride ( $\text{CuCl}_2$ ) and chromium chloride hexahydrate ( $\text{CrCl}_3 \cdot 6\text{H}_2\text{O}$ ) were purchased from Alfa Aesar (Tianjin, China). The water used in all experiments was prepared in a SG water purification system and displayed a resistivity of  $\geq 18.2 \text{ M}\Omega \cdot \text{cm}^{-1}$ . The metal ion stock solutions were prepared in water at concentration of 10 mM and diluted as needed in the fluorescence array experiments.

**General Methods.**  $^1\text{H}$  and  $^{13}\text{C}$  NMR spectra were recorded on a Bruker 400 MHz spectrometer, and chemical shifts were reported in parts per million using tetramethylsilane (TMS) as internal reference. Fluorescence spectra were recorded on a SPEX Fluorolog 3-TCSPC spectrometer with 1 cm path length cuvette, while absorption spectra were recorded on a Beckman DU 800 spectrophotometer. Metal ion arrays were measured on 96-well plates (300  $\mu\text{L}$  Corning) using Tecan M1000 Pro plate reader.

**Data Analysis Method.** Fluorescence intensity of each CPE–metal solution was collected through plate reader. A training matrix (four polymers  $\times$  eight metal ions  $\times$  six replicates) was generated using  $I_0/I$  values for further computational analysis and were processed through LDA using R software. In the analysis, all of the variables were used in the complete mode, and the tolerance was set to 0.001. The raw fluorescence intensity patterns were transformed into canonical score patterns in which the within-class variance to between-class variance was minimized according to preassigned grouping. Canonical scores were calculated by LDA using R software for identification of the eight metal ions.

**Molecular Weight Determination.** All mass spectra were acquired by a 4700 Proteomics Analyzer MALDI-TOF/TOF-MS (Applied Biosystems, Framingham, MA).<sup>35,36</sup> Samples using 2,5-dihydroxybenzoic acid (DHB) as a matrix and AgTFA (trifluoroacetic acid) as an additive were prepared by dissolving the polymer in THF at a concentration of 5 mg/mL. A 5  $\mu\text{L}$  aliquot of this solution was added to a 5  $\mu\text{L}$  aliquot of a 10 mg/mL matrix solution with 1  $\mu\text{L}$  of AgTFA in THF (0.1 M) as the cationization agent. A 1  $\mu\text{L}$  aliquot of the sample solution was hand-spotted on a stainless steel target plate and allowed to dry by air. Samples were analyzed with the operator

manually searching for the sample “sweet spot” for data collection. The samples were measured in negative linear ion mode. All spectra were taken from signal averaging of 300 laser shots. All MS data were further processed using Data Explorer 4.5 (Applied Biosystems).

**Polymer Synthesis.** The backbone of PPEs is synthesized via Sonogashira protocol.<sup>37</sup> In this study, four PPEs with different anionic side groups were obtained. The synthesis of PPE1 and PPE2 were referred to the method previously reported.<sup>38,39</sup>

**Poly(*p*-pheynylene ethynylene)–Iminodiacetate Ester.** A solution of the monomer M1 (162.0 mg, 0.2 mmol) (structure and synthesis in the Supporting Information) and 1,4-diethynylbenzene (25.3 mg, 0.2 mmol) in 20 mL of dry THF/ $\text{Et}_3\text{N}/\text{CH}_2\text{Cl}_2$  ( $v/v/v = 3/1/1$ ) fitted with a condenser were degassed with argon for 15 min. Then 17.4 mg of  $\text{Pd}(\text{PPh}_3)_4$  (15.0  $\mu\text{mol}$ ) and 8 mg of CuI (15.0  $\mu\text{mol}$ ) were added under argon. The reaction mixture was stirred at 60  $^\circ\text{C}$  for 48 h. The obtained reaction solution was poured into 150 mL of cold methanol, and yellow solid was collected and dried (98.3 mg, yield 71%).  $^1\text{H}$  NMR (400 MHz,  $\text{CDCl}_3$ ,  $\delta$ ): 7.5 (d, 4H), 7.1 (d, 4H), 4.8 (t, 4H), 4.1 (m, 16H), 1.2 (m, 12H).

**Poly(*p*-pheynylene ethynylene)–HPA (hexapropanoic acid) Ester.** A solution of the monomers M2 (107.0 mg, 0.1 mmol) and M3 (127.0 mg, 0.1 mmol) (structures and synthesis in the Supporting Information) in 20 mL of dry THF/ $\text{Et}_3\text{N}/\text{CH}_2\text{Cl}_2$  ( $v/v/v = 3/1/1$ ) fitted with a condenser were degassed with argon for 15 min. Then 17.4 mg of  $\text{Pd}(\text{PPh}_3)_4$  (15.0  $\mu\text{mol}$ ) and 8.0 mg of CuI (15.0  $\mu\text{mol}$ ) were added under argon. The reaction mixture was stirred at 60  $^\circ\text{C}$  for 48 h. The obtained reaction solution was poured into 150 mL of cold methanol, and orange solid was collected and dried (59.4 mg, yield 55%).  $^1\text{H}$  NMR (400 MHz,  $\text{CDCl}_3$ ,  $\delta$ ): 7.6 (t, 4H), 7.0 (t, 4H), 6.42 (s, 2H), 4.50 (s, 4H), 2.16 (s, 12H), 1.98 (s, 12H), 1.42 (s, 54H).

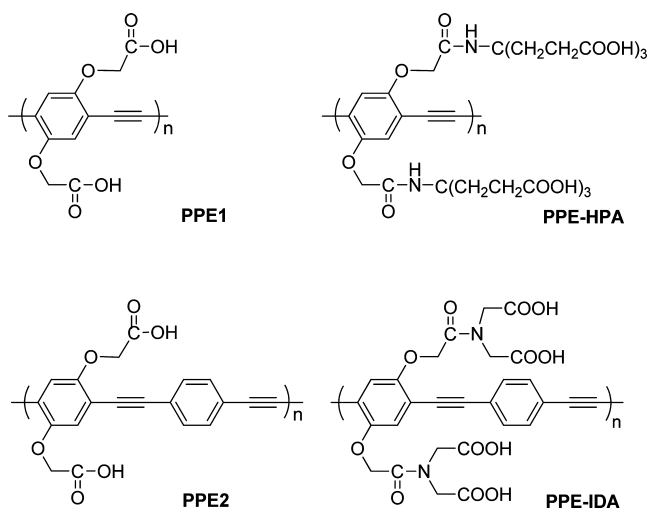
**Poly(*p*-pheynylene ethynylene)–Iminodiacetate.** A solution of PPE–iminodiacetate (IDA) ester (142.0 mg, 0.2 mmol) in 30 mL of dioxane/THF ( $v/v = 5/1$ ) was added to 1.5 mL of 1 M (*n*-Bu) $_4$ NOH in methanol and stirred at room temperature for 24 h. During the course of the hydrolysis, 2 mL of water was systematically added to keep the solution clear. Then a solution of 0.2 g of  $\text{NaIO}_4$  in 3 mL of water was added to the hydrolyzed polymer solution, and the resulting mixture was poured into 400 mL of cold acetone, resulting in the precipitation of PPE–IDA as yellow powders (92.5 mg, yield 76%). The polymer was then dissolved in 50 mL of deionized water (several drops of 1 M NaOH solution were added) and was purified by dialysis against deionized water using a regenerated cellulose membrane (7 kDa molecular weight cutoff). After dialysis, the solution was stored as the stock solution.

**Poly(*p*-pheynylene ethynylene)–hexapropanoic acid.** A solution of PPE–HPA ester (215.0 mg, 0.2 mmol) in 30 mL of dioxane/THF ( $v/v = 5/1$ ) was added to 1.5 mL of 1 M (*n*-Bu) $_4$ NOH in methanol and stirred at room temperature for 24 h. During the course of the hydrolysis reaction, 2 mL of water was systematically added to keep the solution clear. Then a solution of 0.2 g of  $\text{NaIO}_4$  in 3 mL of water was added to the hydrolyzed polymer solution, and the resulting mixture was poured into 400 mL of cold acetone, resulting in the precipitation of PPE–IDA as yellow powders (120.2 mg, yield 82%). The polymer was then dissolved in 50 mL of deionized water (several drops of 1 M NaOH solution were added) and was purified by dialysis against deionized water using a regenerated cellulose membrane (7 kDa molecular weight cutoff). After dialysis, the solution was stored as the stock solution in the refrigerator.

## ■ RESULTS AND DISCUSSION

**Synthesis and Structural Characterization of Conjugated Polyelectrolytes.** CPEs with pendant carboxylate groups have attracted much interest, because of their potential application to the detection of different analytes such as DNAs, cations, proteins, enzymes, and others.<sup>38–41</sup> In this study, two new polymers, PPE–IDA and PPE–HPA, were synthesized together with previously reported polymers PPE1 and PPE2 using Pd-catalyzed Sonogashira coupling, as previously described<sup>37,42</sup> (structures are shown in Scheme 1). In general,

### Scheme 1. Structures of the Four Conjugated Polyelectrolytes, PPE1, PPE2, PPE-IDA, and PPE-HPA



monomeric building blocks of diacetylenes and bis-(iodobenzenes) with different substituents were prepared (see Supporting Information for details on synthesis and structural characterization), followed by polymerization and hydrolysis to construct the final CPEs.

The four polymers shared the same poly(paraphenylene ethynylene) backbone but differed in their repeat unit patterns and side groups: (1) PPE1 and PPE-HPA have two side chains per phenylene-ethynylene unit, whereas PPE2 and PPE-IDA have two side chains for every two phenylene-ethynylene units; (2) PPE1 and PPE2 have the same carboxylate side chains, which have been extensively studied,<sup>40,41,43</sup> whereas PPE-IDA contains special IDA groups, and PPE-HPA contains six propionate groups on the end of each side chain. It is well-known that IDA acts as a metal-chelating agent via metal coordination, especially for Ni<sup>2+</sup> and Cu<sup>2+</sup>.<sup>43</sup> The six propionate groups of PPE-HPA contribute six negative charges to each repeat unit and presumably act to enhance the electrostatic attraction with cationic metal ions. Choosing water-soluble CPEs over other organic molecules as a sensing material for metal ions has an advantage because CPEs do not require the addition of cosolvents to the system.<sup>44</sup>

The molecular weights of the four polymers were determined using matrix-assisted laser desorption ionization (MALDI) mass spectrometry, as shown in Table 1. By using mass spectrometry as a direct molecular weight determination method, this avoids overestimation of average molecular weight ( $\overline{M}_n$ ). Overestimations via traditional gel-permeation chromatography (GPC) are due to the use of flexible polystyrene standards for the analysis of rigid conjugated polymers.<sup>45</sup> Generally, the  $\overline{M}_n$  values fall between 9.8 and 22.5 kDa, while

the weight-average molecular weights ( $\overline{M}_w$ ) fall within a higher range, between 14.6 and 45.6 kDa, resulting in polydispersity indices (PDI) of between  $\sim 1.48$  and 2.04, which is reasonable for step-growth polycondensation.<sup>46</sup>

**Photophysical Characterization of Poly(*p*-phenylene ethynylene)-Based Anionic Polyelectrolytes.** As shown in Figure 1, PPE-IDA and PPE-HPA demonstrated similar

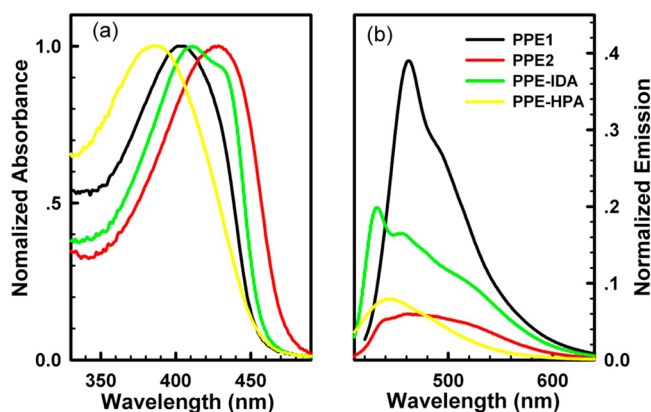


**Figure 1.** UV-visible absorption (a) and fluorescence emission spectra (b) of PPE1 (black), PPE2 (red), PPE-IDA (green) and PPE-HPA (yellow) in aqueous solution. All absorbance and emission spectra were normalized to reflect relative quantum yields.

absorption and emission bands as observed for PPE1 and PPE2. The absorption bands of the four polymers were well-separated, and the maxima ranged from 386 to 429 nm, in the order of PPE-HPA < PPE1 < PPE-IDA < PPE2. This order corresponds to the energy gap between the valence band and conduction band of the polymers. PPE-HPA appeared to have the biggest band gap, because of the shortest conjugation length (only 20 repeat units per polymer chain). Emission spectra show wide bands spanning from 400 to 650 nm. The relative intensities correspond to each polymer's quantum yield, in the order of PPE2 < PPE-HPA < PPE-IDA < PPE1. The differences in the absorption and fluorescence spectra are presumably due to the different conjugation lengths, aggregation states, and side group effects. For example, PPE2 demonstrated the most red-shifted absorption and emission bands with the lowest quantum yield, which is consistent with previous work describing its strong interchain aggregation in aqueous solution. Compared to PPE2, both PPE-IDA and PPE1 showed less aggregation, characterized by their blue-shifted featured absorption bands and stronger fluorescence emission bands. Electronic repulsion between ionic side chains might hinder cofacial stacking of the polymers, leading to less polymer chain aggregation.

**Quenching by Metal Ions.** Eight metal ions, including Pb<sup>2+</sup>, Hg<sup>2+</sup>, Fe<sup>3+</sup>, Cr<sup>3+</sup>, Cu<sup>2+</sup>, Mn<sup>2+</sup>, Ni<sup>2+</sup>, and Co<sup>2+</sup>, were

**Table 1. Characterization Data of the Four Polymers Used in This Study**

polymer	$\overline{M}_n$ ( $\times 10^3$ kDa) <sup>a</sup>	$\overline{M}_w$ ( $\times 10^3$ kDa) <sup>a</sup>	$\overline{x}_n$	PDI	$\lambda_{\max}^{\text{abs}}/\text{nm}$	$\lambda_{\max}^{\text{em}}/\text{nm}$	$\phi_f^b$
PPE1	15.3	24.2	62	1.58	405	463	0.39
PPE2	9.8	14.6	28	1.49	429	462	0.06
PPE-IDA	22.5	45.6	39	2.04	411	432	0.20
PPE-HPA	14.2	21.0	20	1.48	386	444	0.08

<sup>a</sup>Molecular weights were measured on a 4700 Proteomics Analyzer MALDI-TOF/TOF-MS. <sup>b</sup>Quantum yields were measured using coumarin 6 in aqueous solution as a reference, which has a reported quantum yield of 0.78 when excited at 400 nm.



selected as analytes in this study, and are all defined as drinking water contaminants by the United States Environmental Protection Agency (EPA).<sup>47</sup> Sensor arrays possess an advantage in that they can facilitate analysis of a combination of responses instead of just a single response of a given polymer to one specific metal ion. From experimental quenching experiment results (Figure S1 in Supporting Information), it was observed that the four polymers studied here responded in unique ways to addition of metal ions. These distinct responses presumably arise from either the conformational change of the polymers upon interaction with metal ions or are due to a heavy-atom quenching effect (spin–orbit coupling).<sup>48</sup> The response patterns based on the quenching results were visualized by plotting the individual response of each polymer solution upon the addition of metal ions (bar graph, Figure 2). The response

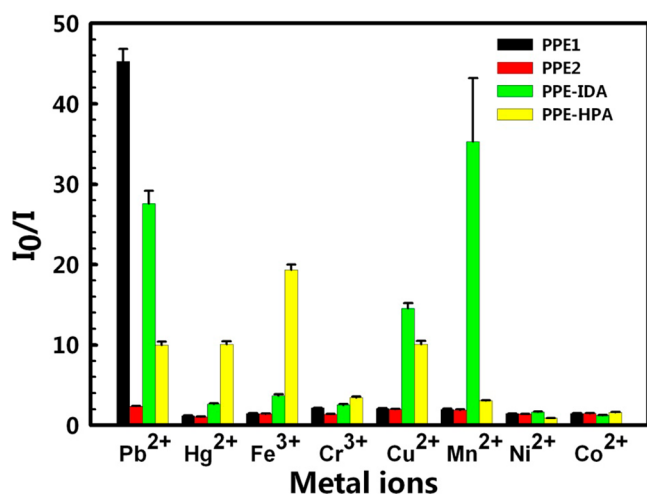


**Figure 2.** Response patterns constructed based on fluorescence quenching of the four polymers by eight metal ions at 5  $\mu\text{M}$  each. The response patterns were generated from the ratios of the initial to the final emission intensities of the polymers. Error bars represent the standard deviations of six replicates for each PPE–metal ion pair. Polymers are PPE1, PPE2, PPE–IDA, and PPE–HPA, and metal ions are  $\text{Pb}^{2+}$ ,  $\text{Hg}^{2+}$ ,  $\text{Fe}^{3+}$ ,  $\text{Cr}^{3+}$ ,  $\text{Cu}^{2+}$ ,  $\text{Mn}^{2+}$ ,  $\text{Ni}^{2+}$ , and  $\text{Co}^{2+}$ .

was calculated as the ratio of fluorescence intensity at emission,  $I_0/I$ , where  $I_0$  and  $I$  are the fluorescence intensities of each CPE without and with metal ions, respectively. Figure 2 demonstrates the response patterns of the array when the concentration of each metal ion was 5  $\mu\text{M}$ . In general, six of the metal ions tested showed appreciable quenching effect levels on some of the polymers, while the VIII group elements  $\text{Ni}^{2+}$  and  $\text{Co}^{2+}$  showed only minimal quenching of all four CPEs at this concentration. By comparing the quenching response of each polymer, we observe that (1) PPE1 showed significant quenching by  $\text{Pb}^{2+}$ , with an  $I_0/I$  value of  $\sim 45.3$ , while all other metal ions exhibited ratios less than 2; (2) PPE2 showed relatively low quenching efficiencies by all eight metal ions, with  $I_0/I$  values between 1.4 and 2.3; (3) PPE–IDA was efficiently quenched by  $\text{Pb}^{2+}$ ,  $\text{Cu}^{2+}$ , and  $\text{Mn}^{2+}$ , with  $I_0/I$  values of 27.6, 14.5, and  $\sim 35.3$ , respectively; and (4) PPE–HPA was appreciably quenched by  $\text{Pb}^{2+}$ ,  $\text{Hg}^{2+}$ ,  $\text{Fe}^{3+}$ , and  $\text{Cu}^{2+}$ , with  $I_0/I$  values from 9.9 to 19.3, while quenching by all other metal ions resulted in ratios less than 3.4.

**Linear Discrimination Analysis and Pattern Construction.** It can be seen from the bar graph that the different metal ions exhibited distinct quenching patterns for the four CPEs.

LDA was performed to further characterize the quenching patterns. LDA is a statistical analysis method that can visually differentiate between two or more kinds of objects or events based on their linear combination of features.<sup>49,50</sup> It has been widely used in array-based sensing of proteins, metal ions, etc.

All metal ions were tested at different concentrations for their effects on the PPEs using six replicate measurements to provide a training matrix of four polymers  $\times$  eight metal ions  $\times$  six replicates. The resulting training data were analyzed and processed through LDA using R software (version i386 3.0.3) and transformed into four canonical scores, which account for 69.1%, 26.7%, 3.5%, and 0.7% of the variation, respectively. The first two factors accounted for 95.8% of the variance and were used to construct the two-dimensional (2-D) discrimination plot, as shown in Figure 3a, where the horizontal and vertical

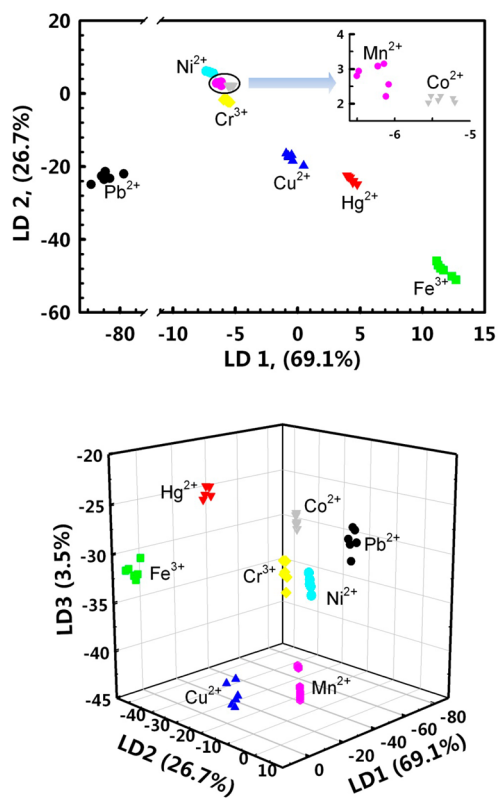


**Figure 3.** 2-D (upper) and 3-D (lower) canonical score plot of the fluorescence response patterns obtained by four-PPE sensor array against eight metal ions at 5  $\mu\text{M}$  concentration.

axes have 69.1% and 26.7% weighting, respectively. Each dot represents the fluorescence response of the four-PPE sensor array to a single metal ion concentration. Clearly, the results for the eight different metal ions are clustered into eight nonoverlapping groups. Especially clear separation can be observed for  $\text{Pb}^{2+}$ ,  $\text{Ni}^{2+}$ ,  $\text{Cr}^{3+}$ ,  $\text{Cu}^{2+}$ ,  $\text{Hg}^{2+}$ , and  $\text{Fe}^{3+}$ , indicating the utility of this method to differentiate these metal ions.  $\text{Mn}^{2+}$  and  $\text{Co}^{2+}$  cluster in close proximity and show overlap along the LD2 axis, but there is still acceptable spatial separation between these two ions along the LD1 axis (as shown in the magnified inset of Figure 3).

Since additional orthogonal dimensions would further enhance separation, a third factor, which exhibits 3.5% variance, was added to the first two factors to build a three-dimensional (3-D) pattern (Figure 3, lower). The eight metal ions, including

even the previously poorly discriminated  $\text{Mn}^{2+}$  and  $\text{Co}^{2+}$ , were well-separated into eight clusters with excellent spatial resolution on the 3-D plot, which shows better resolution than that of the 2-D plot.

Patterns at lower metal ion concentrations, including 100 nM, 500 nM, 1  $\mu\text{M}$ , and 2  $\mu\text{M}$ , were further analyzed using the same procedures to examine the sensitivity of this method. As shown in Supporting Information, Figure S2, 2-D patterns could differentiate among six of the metal ions with acceptable resolution, even when the concentration of each metal ion was as low as 100 nM, except  $\text{Mn}^{2+}$  and  $\text{Co}^{2+}$ , which were merged to some extent. However, in the 3-D patterns, these two metal ions could be differentiated to an acceptable level of resolution, as shown in Supporting Information, Figure S3. These results indicate that higher sensitivity could be achieved by using the combination of 2-D and 3-D discriminant patterns.

To explore the potential application of this array to metal ion analysis, we tested the four-PPE sensor array to quantify metal ions in aqueous solution.  $\text{Pb}^{2+}$  and  $\text{Hg}^{2+}$  were chosen because they are serious environmental contaminants that are well-discriminated by the array. We plotted calibration curves using the fluorescence intensity ratios ( $I_0/I$ ) from the four-PPE sensor array at various concentrations of  $\text{Pb}^{2+}$  and  $\text{Hg}^{2+}$  in water. Figure 4 shows the concentration curve of  $\text{Pb}^{2+}$  and  $\text{Hg}^{2+}$

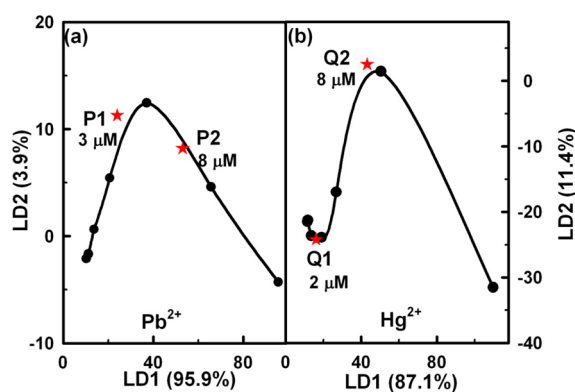


**Figure 4.** Canonical score plot of the first two factors of fluorescence response patterns obtained through the four-PPE sensor array with various concentrations of  $\text{Pb}^{2+}$  (a) and  $\text{Hg}^{2+}$  (b) in water. The concentrations tested are noted on the figure. P1 (3  $\mu\text{M}$ ) and P2 (8  $\mu\text{M}$ ) represent the data obtained from blind samples of  $\text{Pb}^{2+}$ , whereas Q1 (2  $\mu\text{M}$ ) and Q2 (8  $\mu\text{M}$ ) represent the data obtained from blind samples of  $\text{Hg}^{2+}$ .

plotted against the canonical scores obtained from the LDA. The concentration curves show that the four-PPE sensor array dynamically responded to  $\text{Pb}^{2+}$  and  $\text{Hg}^{2+}$  in the range of 100 nM to 20  $\mu\text{M}$ . Results from blind samples containing unknown amounts of  $\text{Pb}^{2+}$  and  $\text{Hg}^{2+}$  were obtained and plotted alongside the concentration curves to estimate the concentrations of these metal ions (P1 and P2 in Figure 4a; Q1 and Q2 in Figure 4b). As indicated in Figure 4, all of the four unknown samples were quantified by interpolation with good accuracy.

## CONCLUSION

In conclusion, we have demonstrated effective fluorescence array-based sensing of metal ions using a four-PPE sensor array, which affords very good differentiation between eight metal ions, as evidenced by clearly separated data clusters in both 2-D and 3-D LDA plots. The diverse fluorescence responses of the

PPEs toward metal ions depends on the unique structures of polymers used in the sensor array. In particular, such an array could readily differentiate between eight toxic metal ions in aqueous solution, each analyzed separately at 100 nM, by examining both 2-D and 3-D discriminant patterns. Such concentration levels are below the threshold levels of detection as defined in the EPA standards (Supporting Information, Table S1). The current approach demonstrates advantages over other methods by including environmentally friendly fluorescent materials, simple sample preparation and measurements, as well as convenient data processing and a straightforward pattern analysis procedure. In our ongoing studies, we are exploiting strategies to expand this approach for use in detection of combinations of toxic metal ions, as well as exploring a larger repertoire of metal contaminants.

## ASSOCIATED CONTENT

### Supporting Information

Monomer synthesis, NMR spectra, quenching data of four polymers by different metal ions, and 2-D and 3-D patterns of metal ions at lower concentrations, EPA fresh water quality standard. This material is available free of charge via the Internet at <http://pubs.acs.org>.

## AUTHOR INFORMATION

### Corresponding Authors

\*Phone: 86-755-26036533. Fax: 86-755-26032094. E-mail: [tancy@sz.tsinghua.edu.cn](mailto:tancy@sz.tsinghua.edu.cn). (C.T.)

\*E-mail: [jiangyy@sz.tsinghua.edu.cn](mailto:jiangyy@sz.tsinghua.edu.cn). (Y.J.)

### Notes

The authors declare no competing financial interest.

## ACKNOWLEDGMENTS

The authors are thankful for the financial support from the Ministry of Science and Technology of China (MOSTC 2012ZX09506001-010) and Shenzhen Municipal Government SZSITIC (JCYJ20130402145002384 and ZDSY2012061914142872). Also C.T. would like to thank Prof. P. Yang at Fudan Univ. for his help with molecular weight determination of CPEs with mass spectrometer.

## REFERENCES

- (1) Nriagu, J. O. A History of Global Metal Pollution. *Science* **1996**, *272*, 223.
- (2) Pohl, P. Determination of Metal Content in Honey by Atomic Absorption and Emission Spectrometries. *TrAC, Trends Anal. Chem.* **2009**, *28*, 117–128.
- (3) Karunasagar, D.; Arunachalam, J. Determination of Cadmium by Inductively Coupled Plasma Mass Spectrometry-Reduction of Molybdenum Oxide Interferences by Addition of Acetonitrile. *Anal. Chim. Acta* **2001**, *441*, 291–296.
- (4) Miranda, O. R.; You, C.-C.; Phillips, R.; Kim, I.-B.; Ghosh, P. S.; Bunz, U. H. F.; Rotello, V. M. Array-Based Sensing of Proteins Using Conjugated Polymers. *J. Am. Chem. Soc.* **2007**, *129*, 9856–9857.
- (5) Jagt, R. B. C.; Gómez-Biagi, R. F.; Nitz, M. Pattern-Based Recognition of Heparin Contaminants by an Array of Self-Assembling Fluorescent Receptors. *Angew. Chem., Int. Ed.* **2009**, *121*, 2029–2031.
- (6) Margulies, D.; Hamilton, A. D. Protein Recognition by an Ensemble of Fluorescent DNA G-Quadruplexes. *Angew. Chem., Int. Ed.* **2009**, *121*, 1803–1806.
- (7) Lin, H.; Jang, M.; Suslick, K. S. Preoxidation for Colorimetric Sensor Array Detection of VOCs. *J. Am. Chem. Soc.* **2011**, *133*, 16786–16789.

- (8) Bajaj, A.; Miranda, O. R.; Phillips, R.; Kim, I.-B.; Jerry, D. J.; Bunz, U. H. F.; Rotello, V. M. Array-Based Sensing of Normal, Cancerous, and Metastatic Cells Using Conjugated Fluorescent Polymers. *J. Am. Chem. Soc.* **2009**, *132*, 1018–1022.
- (9) Zhang, C.; Suslick, K. S. Colorimetric Sensor Array for Soft Drink Analysis. *J. Agric. Food Chem.* **2006**, *55*, 237–242.
- (10) Kwon, H.; Samain, F.; Kool, E. T. Fluorescent DNAs Printed on Paper: Sensing Food Spoilage and Ripening in the Vapor Phase. *Chem. Sci.* **2012**, *3*, 2542–2549.
- (11) Mayr, T.; Igel, C.; Liebsch, G.; Klimant, I.; Wolfbeis, O. S. Cross-Reactive Metal Ion Sensor Array in a Micro Titer Plate Format. *Anal. Chem.* **2003**, *75*, 4389–4396.
- (12) Hewage, H. S.; Anslyn, E. V. Pattern-Based Recognition of Thiols and Metals Using a Single Squaraine Indicator. *J. Am. Chem. Soc.* **2009**, *131*, 13099–13106.
- (13) Yuen, L. H.; Franzini, R. M.; Wang, S.; Crisalli, P.; Singh, V.; Jiang, W.; Kool, E. T. Pattern-Based Detection of Toxic Metals in Surface Water with DNA Polyfluorophores. *Angew. Chem., Int. Ed.* **2014**, *53*, 5361–5365.
- (14) An, L.; Liu, L.; Wang, S. Label-Free, Homogeneous, and Fluorescence “Turn-On” Detection of Protease Using Conjugated Polyelectrolytes. *Biomacromolecules* **2008**, *10*, 454–457.
- (15) Liu, Y.; Schanze, K. S. Conjugated Polyelectrolyte Based Real-Time Fluorescence Assay for Adenylate Kinase. *Anal. Chem.* **2008**, *81*, 231–239.
- (16) McQuade, D. T.; Pullen, A. E.; Swager, T. M. Conjugated Polymer-Based Chemical Sensors. *Chem. Rev.* **2000**, *100*, 2537–2574.
- (17) Pu, K.-Y.; Liu, B. Intercalating Dye Harnessed Cationic Conjugated Polymer for Real-Time Naked-Eye Recognition of Double-Stranded DNA in Serum. *Adv. Funct. Mater.* **2009**, *19*, 1371–1378.
- (18) Thomas, S. W.; Joly, G. D.; Swager, T. M. Chemical Sensors Based on Amplifying Fluorescent Conjugated Polymers. *Chem. Rev.* **2007**, *107*, 1339–1386.
- (19) Wosnick, J. H.; Mello, C. M.; Swager, T. M. Synthesis and Application of Poly(phenylene Ethynylene)s for Bioconjugation: A Conjugated Polymer-Based Fluorogenic Probe for Proteases. *J. Am. Chem. Soc.* **2005**, *127*, 3400–3405.
- (20) Zhou, Q.; Swager, T. M. Method for Enhancing the Sensitivity of Fluorescent Chemosensors: Energy Migration in Conjugated Polymers. *J. Am. Chem. Soc.* **1995**, *117*, 7017–7018.
- (21) Chen, L.; McBranch, D. W.; Wang, H.-L.; Helgeson, R.; Wudl, F.; Whitten, D. G. Highly Sensitive Biological and Chemical Sensors Based on Reversible Fluorescence Quenching in a Conjugated Polymer. *Proc. Natl. Acad. Sci. U. S. A.* **1999**, *96*, 12287–12292.
- (22) Levitsky, I. A.; Kim, J.; Swager, T. M. Energy Migration in a Poly(phenylene ethynylene): Determination of Interpolymer Transport in Anisotropic Langmuir–Blodgett Films. *J. Am. Chem. Soc.* **1999**, *121*, 1466–1472.
- (23) Wu, D.; Schanze, K. S. Protein Induced Aggregation of Conjugated Polyelectrolytes Probed with Fluorescence Correlation Spectroscopy: Application to Protein Identification. *ACS Appl. Mater. Interfaces* **2014**, *6*, 7646–7651.
- (24) Gaylord, B. S.; Heeger, A. J.; Bazan, G. C. DNA Hybridization Detection with Water-Soluble Conjugated Polymers and Chromophore-Labeled Single-Stranded DNA. *J. Am. Chem. Soc.* **2003**, *125*, 896–900.
- (25) Liu, B.; Bazan, G. C. Homogeneous Fluorescence-Based DNA Detection with Water-Soluble Conjugated Polymers. *Chem. Mater.* **2004**, *16*, 4467–4476.
- (26) Chi, C.; Mikhailovsky, A.; Bazan, G. C. Design of Cationic Conjugated Polyelectrolytes for DNA Concentration Determination. *J. Am. Chem. Soc.* **2007**, *129*, 11134–11145.
- (27) He, F.; Tang, Y.; Yu, M.; Wang, S.; Li, Y.; Zhu, D. Fluorescence-Amplifying Detection of Hydrogen Peroxide with Cationic Conjugated Polymers, and Its Application to Glucose Sensing. *Adv. Funct. Mater.* **2006**, *16*, 91–94.
- (28) Bajaj, A.; Miranda, O. R.; Kim, I.-B.; Phillips, R. L.; Jerry, D. J.; Bunz, U. H.; Rotello, V. M. Detection and Differentiation of Normal, Cancerous, and Metastatic Cells Using Nanoparticle-Polymer Sensor Arrays. *Proc. Natl. Acad. Sci. U. S. A.* **2009**, *106*, 10912–10916.
- (29) Bunz, U. H. F.; Rotello, V. M. Gold Nanoparticle–Fluorophore Complexes: Sensitive and Discerning “Noses” for Biosystems Sensing. *Angew. Chem., Int. Ed.* **2010**, *49*, 3268–3279.
- (30) De, M.; Rana, S.; Akpinar, H.; Miranda, O. R.; Arvizo, R. R.; Bunz, U. H. F.; Rotello, V. M. Sensing of Proteins in Human Serum Using Conjugates of Nanoparticles and Green Fluorescent Protein. *Nat. Chem.* **2009**, *1*, 461–465.
- (31) Phillips, R. L.; Miranda, O. R.; You, C.-C.; Rotello, V. M.; Bunz, U. H. F. Rapid and Efficient Identification of Bacteria Using Gold-Nanoparticle–Poly(*para*-phenyleneethynylene) Constructs. *Angew. Chem., Int. Ed.* **2008**, *47*, 2590–2594.
- (32) You, C.-C.; Miranda, O. R.; Gider, B.; Ghosh, P. S.; Kim, I.-B.; Erdogan, B.; Krovci, S. A.; Bunz, U. H. F.; Rotello, V. M. Detection and Identification of Proteins Using Nanoparticle-Fluorescent Polymer “Chemical Nose” Sensors. *Nat. Nanotechnol.* **2007**, *2*, 318–323.
- (33) Zhu, C.; Yang, Q.; Liu, L.; Wang, S. Visual Optical Discrimination and Detection of Microbial Pathogens Based on Diverse Interactions of Conjugated Polyelectrolytes with Cells. *J. Mater. Chem.* **2011**, *21*, 7905–7912.
- (34) Xu, H.; Wu, W.; Chen, Y.; Qiu, T.; Fan, L.-J. Construction of Response Patterns for Metal Cations by Using a Fluorescent Conjugated Polymer Sensor Array from Parallel Combinatorial Synthesis. *ACS Appl. Mater. Interfaces* **2014**, *6*, 5041–5049.
- (35) Brandt, H.; Ehmman, T.; Otto, M. Investigating the Effect of Mixing Ratio on Molar Mass Distributions of Synthetic Polymers Determined by MALDI-TOF Mass Spectrometry Using Design of Experiments. *J. Am. Soc. Mass Spectrom.* **2010**, *21*, 1870–1875.
- (36) Weidner, S.; Knappe, P.; Panne, U. MALDI-TOF Imaging Mass Spectrometry of Artifacts in “Dried Droplet” Polymer Samples. *Anal. Bioanal. Chem.* **2011**, *401*, 127–134.
- (37) Zhao, X.; Pinto, M. R.; Hardison, L. M.; Mwaura, J.; Müller, J.; Jiang, H.; Witker, D.; Kleiman, V. D.; Reynolds, J. R.; Schanze, K. S. Variable Band Gap Poly(arylene ethynylene) Conjugated Polyelectrolytes. *Macromolecules* **2006**, *39*, 6355–6366.
- (38) Haskins-Glusac, K.; Pinto, M. R.; Tan, C.; Schanze, K. S. Luminescence Quenching of a Phosphorescent Conjugated Polyelectrolyte. *J. Am. Chem. Soc.* **2004**, *126*, 14964–14971.
- (39) Lee, S. H.; Kömürlü, S.; Zhao, X.; Jiang, H.; Moriena, G.; Kleiman, V. D.; Schanze, K. S. Water-Soluble Conjugated Polyelectrolytes with Branched Polyionic Side Chains. *Macromolecules* **2011**, *44*, 4742–4751.
- (40) Liu, R.; Tan, Y.; Zhang, C.; Wu, J.; Mei, L.; Jiang, Y.; Tan, C. A Real-Time Fluorescence Turn-on Assay for Trypsin Based on a Conjugated Polyelectrolyte. *J. Mater. Chem. B* **2013**, *1*, 1402–1405.
- (41) Wu, J.; Tan, Y.; Xie, Y.; Wu, Y.; Zhao, R.; Jiang, Y.; Tan, C. Diazobenzene-Containing Conjugated Polymers as Dark Quenchers. *Chem. Commun.* **2013**, *49*, 11379–11381.
- (42) Suda, Y.; Arano, A.; Fukui, Y.; Koshida, S.; Wakao, M.; Nishimura, T.; Kusumoto, S.; Sobel, M. Immobilization and Clustering of Structurally Defined Oligosaccharides for Sugar Chips: an Improved Method for Surface Plasmon Resonance Analysis of Protein-Carbohydrate Interactions. *Bioconjugate Chem.* **2006**, *17*, 1125–1135.
- (43) Fan, H.; Zhang, T.; Lv, S.; Jin, Q. Fluorescence Turn-on Assay for Glutathione Reductase Activity Based on a Conjugated Polyelectrolyte with Multiple Carboxylate Groups. *J. Mater. Chem.* **2010**, *20*, 10901–10907.
- (44) Szurdoki, F.; Ren, D.; Walt, D. R. A Combinatorial Approach To Discover New Chelators for Optical Metal Ion Sensing. *Anal. Chem.* **2000**, *72*, 5250–5257.
- (45) Gies, A. P.; Geibel, J. F.; Hercules, D. M. MALDI-TOF MS Study of Poly(*p*-phenylene sulfide). *Macromolecules* **2009**, *43*, 943–951.
- (46) Yokozawa, T.; Asai, T.; Sugi, R.; Ishigooka, S.; Hiraoka, S. Chain-Growth Polycondensation for Nonbiological Polyamides of Defined Architecture. *J. Am. Chem. Soc.* **2000**, *122*, 8313–8314.

(47) EPA, "National Recommended Water Quality Criteria", can be found online at <http://water.epa.gov/scitech/swguidance/standards/criteria/current/index.cfm> (accessed on Jan. 17, 2015).

(48) Gorman, A.; Killoran, J.; O'Shea, C.; Kenna, T.; Gallagher, W. M.; O'Shea, D. F. In Vitro Demonstration of the Heavy-Atom Effect for Photodynamic Therapy. *J. Am. Chem. Soc.* **2004**, *126*, 10619–10631.

(49) Jurs, P.; Bakken, G.; McClelland, H. Computational Methods for the Analysis of Chemical Sensor Array Data from Volatile Analytes. *Chem. Rev.* **2000**, *100*, 2649–2678.

(50) Lu, J.; Plataniotis, K. N.; Venetsanopoulos, A. N. Regularization Studies of Linear Discriminant Analysis in Small Sample Size Scenarios with Application to Face Recognition. *Pattern Recognit. Lett.* **2005**, *26*, 181–191.